



Investigating Effect of CdS Buffer Layer on the Performance of $\text{Cu}_2\text{ZnSnS}_4$ Based Solar Cells Using SCAPS-1D

Rihana Khan¹ · Sumair Faisal Ahmed¹ · Muhammad Khalid¹ · Bhawana Joshi²

Received: 25 October 2019 / Revised: 8 July 2020 / Accepted: 23 July 2020 / Published online: 5 August 2020
© The Korean Institute of Electrical and Electronic Material Engineers 2020

Abstract

Enhancement in performance of Copper Zinc Tin Sulphide ($\text{Cu}_2\text{ZnSnS}_4$) based thin film solar cell has been proposed using SCAPS-1D simulation program. The proposed cell structure $\text{Cu}_2\text{ZnSnS}_4$ (CZTS) included CdS as buffer layer, CZTS as absorber layer, and n-doped ZnO as window layer. On these layers, the open circuit voltage (V_{oc}), short circuit current density (J_{sc}), fill factor (FF), conversion efficiency (η), and quantum efficiency (QE) have been examined at the effect of temperature (280–400 K), thickness (500–4000 nm) series ($1 \Omega \text{ cm}^2$) and shunt ($1000 \Omega \text{ cm}^2$) resistances. The performance of proposed cell has been improved in terms of QE, J_{sc} , V_{oc} , η , and QE with respect to the standard Mo/ $\text{Cu}_2\text{ZnSnS}_4$ /CdS/ZnO solar cell. However, by optimizing, we have successfully achieved the enhancement in efficiency of 19.64%, while J_{sc} , V_{oc} , and FF are 24.22 mA cm^{-2} , 0.9489 V, and 86.13% were observed, respectively.

Keywords CZTS · SCAPS-1D · Thin film solar cell · Electrical properties

1 Introduction

Current challenges in the field of photovoltaic (PV) area is to fabricate the solar cells with low cost, high efficiency, good stability, mass production, without deteriorating materials property [1]. Recently, many researchers draw attention on the Copper Zinc Tin Sulphide (CZTS) ($\text{Cu}_2\text{ZnSnS}_4$) based thin-film solar cells due to so many reason [2–4]. Some of them are, (1) CZTS has excellent PV properties such as direct band gap (1.4–1.5 eV) that is near to value of optimal band gap, (2) high absorption coefficient ($\sim 10^4 \text{ cm}^{-1}$), and (3) CZTS based solar cells are gradually becoming excellent low cost than other solar cells [5]. The main advantages of CZTS based solar cells are the high band gap value of absorber layer and window layer. Cadmium Sulphide

(CdS) used as a buffer layer. Theoretically, the solar cell fabricated using CdS as buffer layer provided a good performance. However, in experimental work, deposited CdS layer gives lower performance than theoretical [6]. Moreover, buffer layer of CdS is necessary to protect the absorber layer from overheating. And, buffer layer creates junction with absorber layer, thereby improves bulk recombination of the solar cell. Generally, other parameters such as temperature, shunt resistances (R_{sh}) and series resistance (R_s) are factors limiting the overall performance of CZTS solar cells [7]. Besides, research on experimental studies of thin film solar cell and simulation techniques are an effective way to study the effects of change in solar cell properties. Thereafter, solar cell can be optimized before fabricating the solar cell. Simulation of CZTS/CdS heterojunction solar cells are available elsewhere [8]. SCAPS-1D simulation software has been used to simulate the electrical characteristics viz. direct current (dc) and alternating current (ac) of CdTe, CZTS and CIGS solar cells. It also permits to characterize solar cells through quantum efficiency (QE) and current–voltage (J – V). Furthermore, QE and J – V characteristics permits us to detect the losses of current by reflection and recombination in the different layer, which are very useful to optimize the performance of PV module [9].

In this manuscript, performance of Mo/ $\text{Cu}_2\text{ZnSnS}_4$ /CdS/ZnO solar cells through J – V and quantum efficiency QE (λ)

✉ Rihana Khan
rihanakhan788@gmail.com

✉ Sumair Faisal Ahmed
sumair.eienano@gmail.com

Muhammad Khalid
mkhalid8406@gmail.com

¹ Central Instrumentation Facility (CIF), Jamia Millia Islamia, Jamia Nagar, New Delhi 110025, India

² Department of Applied Physics, Gautam Buddha University, Greater Noida, U.P 201310, India

characteristics has been studied here. Furthermore, the effect of CZTS absorber layer thickness, temperature, and series and shunt resistances on the electronics and electrical performance of the proposed solar cell has been studied here.

2 Device Structure and Numerical Simulation

The purposed device structure for CZTS solar cell for the present study is shown in Fig. 1. It was constituted by four semi-conductor layers and two metallic contact layers. Soda lime glass (SLG) is considered as the substrate which is the support of the device. Diffusion of sodium coming from the substrate in the CZTS improves the performances of the solar cells. This enhancement was mainly due to higher fill factor (FF) and open circuit voltage (Voc) by increasing hole density and film conductivity.

In the proposed structure, there are three important layers such as window layer (n-ZnO), buffer layer (CdS), and absorber layer (CZTS). CZTS is most vital element of solar device, having direct band gap of 1.5 eV. CZTS band gap energy is near to the value of the sunlight spectrum absorption which is situated at 1.4 eV. CdS is a n-type semiconductor layer with direct band gap of 2.4 eV. It is p-type conductivity layer inside which photons are converted to electron–hole pairs. Cadmium diffuses into CZTS layer, forming a n-type region. Cadmium doping plays a vital role in the creation of p–n junction inside the absorber layer. In the present study, deposition of CdS layer was followed by ZnO layer. ZnO has a wide direct band gap of 3.37 eV. This ZnO layer allows a maximum number of photons to reach the CZTS layer. Between

the substrate and CZTS layer, there is a molybdenum (Mo) layer. It is back contact and useful for holes collection. Finally, the front contact collects the electrons and is generally constituted by nickel/aluminum.

Numerical simulation is an important tool for the characterization of PV cells. It has the benefit to control whole device and material properties. Numerical simulation enables us to add the input parameters in the model and to quantify changes in current–voltage (J–V) or quantum efficiency [QE (λ)] trends. One of several software is SCAPS-1D, which is better in performance than analysis of silicon amorphous (ASA), photonic computer one dimension (PC-1D), AFORS-HET (program for simulation of heterojunction PV cell), review of microelectronic, photonic structures one-dimension (AMPS-1D), and so on. Furthermore, SCAPS-1D is widely used for the simulation of CIGS and CdTe based thin film solar cells and it was developed in University of Gent [10]. It has been developed in order to simulate the functioning of different PV cell structures.

From literature review, good compatibility between SCAPS-1D simulation results and the existing experimental results motivated us to use this tool in the present work [11]. The brief theory behind this software is discussed below.

SCAPS-1D simulation software calculates the solution of the basic semi-conductor equations in one dimension and in steady state conditions. Poisson's equation for electrostatic potential, and continuity equations for electron and holes with the approximate boundary conditions [12].

Poisson's equation used for semiconductor is given as:

$$\nabla \cdot \epsilon \nabla \varphi = -q(p - n + N_D^+ - N_A^-) \quad (1)$$

And the continuity equations for electron and holes are, respectively:

$$\nabla \cdot J_n = q(R - G) + q \frac{\partial n}{\partial t} \quad (2)$$

$$\nabla \cdot J_p = -q(R - G) + q \frac{\partial p}{\partial t} \quad (3)$$

where ϵ is the dielectric constant, φ is the electrostatic potential, n and p are the free carrier concentrations for electron and holes, respectively. N_D^+ and N_A^- are the density of ionized donor and acceptor, J_n and J_p are the electron and hole current density, R and G is the recombination and generation rate, respectively.

In a case of stationary condition, we have:

$$\frac{\partial n}{\partial t} = \frac{\partial p}{\partial t} = 0 \quad (4)$$

Therefore, Eqs. (2) and (3) become as follows:

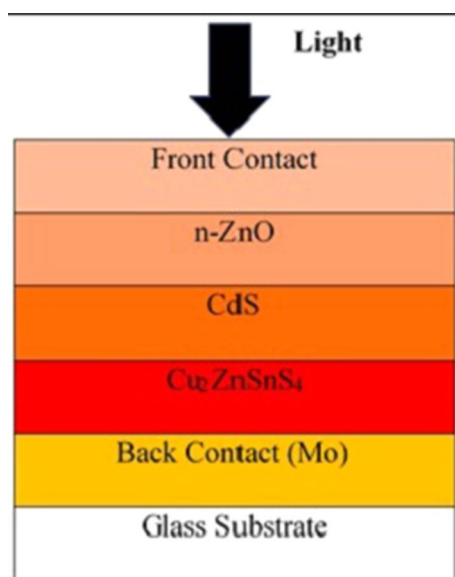


Fig. 1 Schematic structure of CZTS solar cell

$$\nabla \cdot J_n = q(R - G) \tag{5}$$

$$\nabla \cdot J_p = -q(R - G) \tag{6}$$

The recombination and generation term in Eqs. (5) and (6) has non-linear dependencies on the charge carrier concentrations i.e. n and p. The simulation software use Fermi–Dirac statistics for the simulation and which is given by the following Eq. (7)

$$f(E) = \frac{1}{\left(1 + \exp\left[\frac{(E-E_f)}{KT}\right]\right)} \tag{7}$$

where E, E_f , k and T are the energy level of particle, equilibrium Fermi level energy, Boltzmann constant absolute temperature, respectively.

In the present work, all simulations of thin film solar cell have been performed by considering AM 1.5 solar light spectrum with an incident power density of 100 mW cm⁻².

3 Results and Discussions

The effects of operating temperature, absorber layer thickness, series and shunt resistances are discussed in the subsequent sections. The input parameters of different layers which are required for the simulation of the CZTS solar cell performance are summarized in the following Table 1.

3.1 Impact of the Operating Temperature on the Thin Film Solar Cell Performance

Current density (J)–Voltage (V) and Quantum Efficiency (QE)–Wavelength (λ) curves has been shown in Fig. 2a and

Table 1 Material parameters used in the simulation [13]

Material properties	Absorber layer (CZTS)	Buffer layer (CdS)	TCO layer (n-ZnO)
Thickness (μm)	2	0.05	0.2
Energy band gap (eV)	1.5	2.4	3.3
Electron affinity (eV)	4.5	4.5	4.6
Dielectric permittivity	10	9	9
CB effective density of state (cm ⁻³)	2.2 × 10 ¹⁸	1.8 × 10 ¹⁹	2.2 × 10 ¹⁸
VB effective density of state (cm ⁻³)	1.8 × 10 ¹⁹	2.4 × 10 ¹⁸	1.8 × 10 ¹⁹
Electron thermal velocity (cm s ⁻¹)	1 × 10 ⁷	1 × 10 ⁷	1 × 10 ⁷
Hole thermal velocity (cm s ⁻¹)	1 × 10 ⁷	1 × 10 ⁷	1 × 10 ⁷
Electron mobility (cm ² V ⁻¹ s ⁻¹)	100	3.5 × 10 ²	100
Hole mobility (cm ² V ⁻¹ s ⁻¹)	25	50	25
Donor density ND (cm ⁻³)	100	1 × 10 ¹⁷	1 × 10 ¹⁸
Acceptor density NA (cm ⁻³)	2 × 10 ⁴	1 × 10 ⁵	1 × 10 ⁵

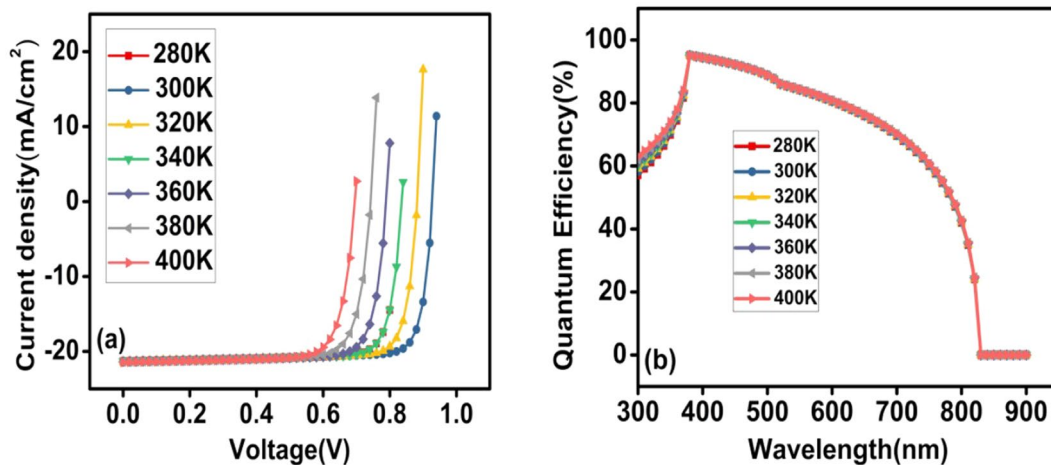


Fig. 2 a Current density (J)–voltage (V) and b quantum efficiency (QE)–wavelength (λ) curves according to different operating temperature

b, respectively. Here, we have varied temperature from 280 to 400 K with the ramp rate of 20 K. It is worth to mention here that the working temperature plays a significant part in the overall performance of the solar cells. Sunlight causes heating of the PV panels, thus there is rise in temperature of PV cells. From Fig. 2, it was observed that the overall cell performance decreases with increase in operating temperature. This was due to as the temperature increases; there will be decrease in band gap of PV cell thus open circuit voltage decreases. At higher temperature, the other parameters such as band gap of the materials, carrier concentrations, and electron and hole mobility also get affected. This in-turn results in lower solar cell efficiency.

Figure 3 shows graph of V_{oc} , J_{sc} , fill factor (FF) and quantum efficiency versus temperature. It can be observed that when the temperature was increased, the open circuit voltage decreases, and short circuit current density

increases. Increase in short circuit current density was due to formation of semiconductor material [14]. This will affect the overall FF and quantum efficiency of PV cell. It was found that at 280 K, the efficiency of thin film solar cell was maximum than other light generated electrons or carriers. Actually, short circuit current of PV cell depends on semiconductor material [14]. This will affect the overall FF and quantum efficiency of PV cell. It was found that at 280 K, the efficiency of thin film solar cell was maximum than other temperatures.

3.2 Effect of CZTS Absorber Layer Thickness on the Solar Cell Performance

Effect of CZTS absorber layer thickness on solar cell performance has presented in Figs. 4 and 5. Figure 4 shows J–V characteristics and QE curves of CZTS based solar cell of

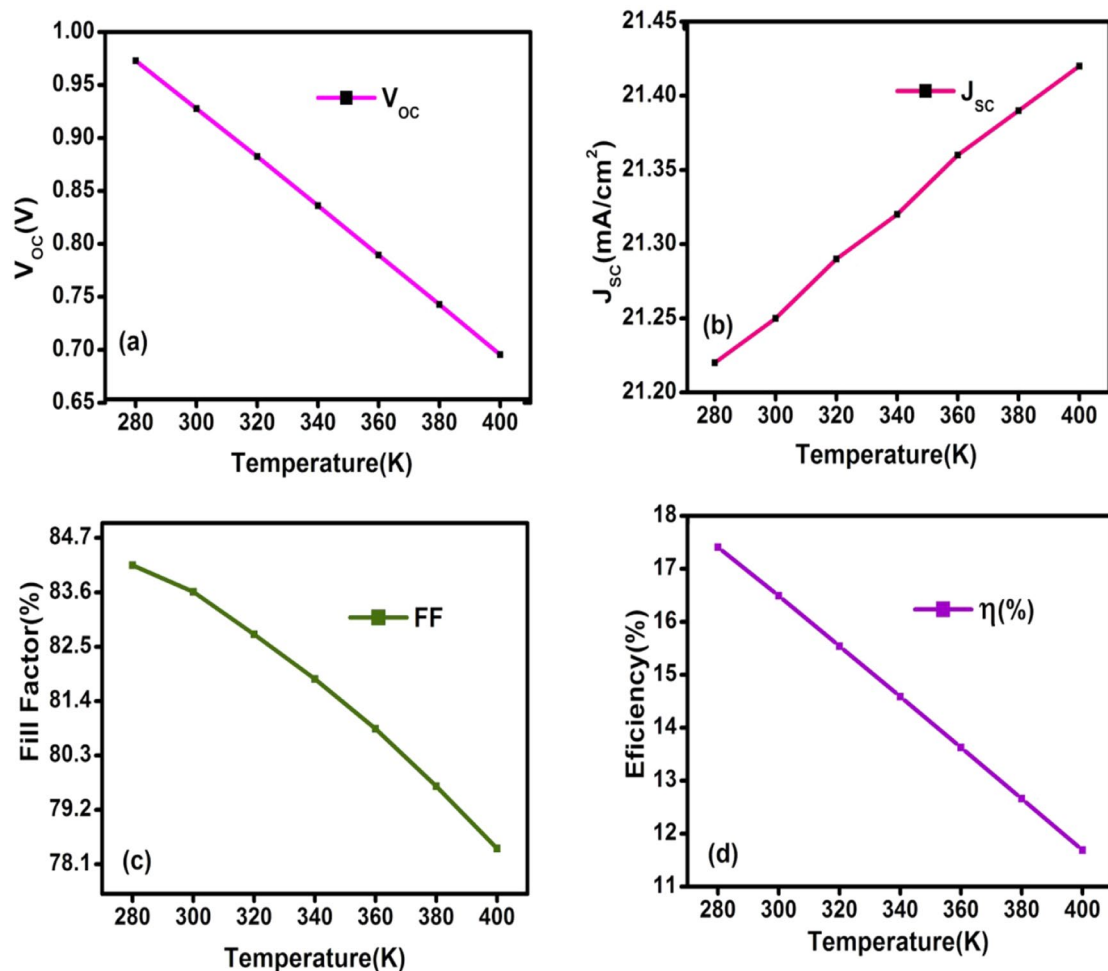


Fig. 3 a Temperature effect on the cell V_{oc} , b temperature thickness effect on the cell J_{sc} , c temperature effect on the cell FF, and d temperature effect on the cell η

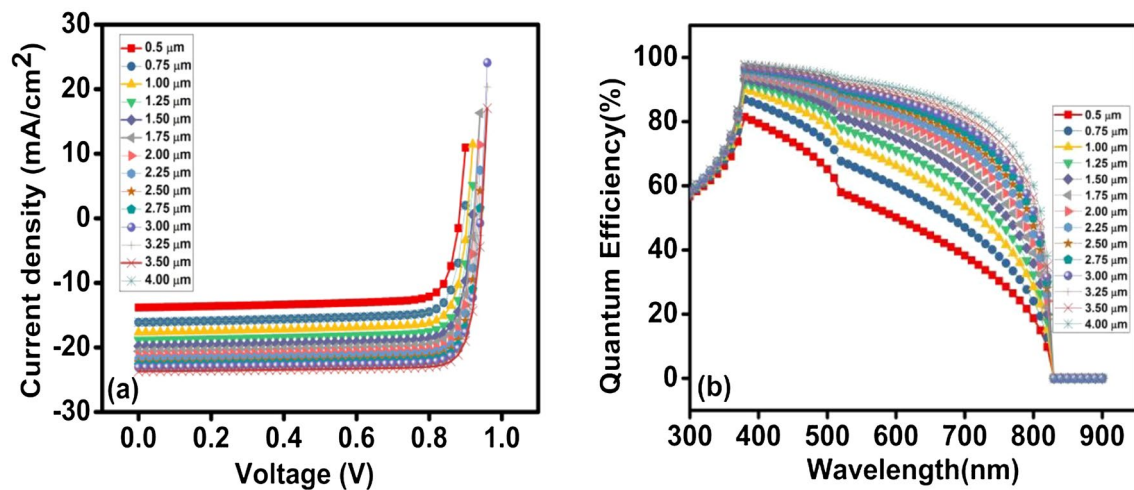


Fig. 4 **a** Current density (J)–voltage (V) and **b** quantum efficiency (QE)–wavelength (λ) curves according to different absorber layer thickness

various thickness. Figure 5 represents (a) CZTS thickness effect on the cell V_{oc} , (b) CZTS thickness effect on the cell J_{sc} , (c) CZTS layer thickness effect on the cell FF, and (d) CZTS layer thickness effect on the cell η .

Thickness of CZTS layer was varied from 500 to 4000 nm. While other material parameters of different layers are kept unchanged [15]. From Fig. 5, it was found that current density (J_{sc}), open circuit voltage (V_{oc}), fill factor, and the efficiency (η) of the solar cell were increased with the increasing thickness of CZTS layer. Highest efficiency is found at 19.64% having CZTS thickness of 4 μm . This was mainly because of the reason that the thicker absorber layer will absorb a greater number of photons with longer wavelengths, which in turn will make a contribution to the generation of electron–hole pairs. Rahman et al. [2] had obtained an efficiency of 14.4% for CdS/CZTS solar cells having CZTS thickness of 5 μm . However, almost a linear increase of J_{sc} has obtained, when the CZTS layer thickness was less than 1000 nm, which can be mainly attributed to the complete absorption of the incident photons and increasing recombination of photo-generated carriers at the back contact which is located near the depletion region in a cell with thin absorber layer. Thus, less photo-generated electrons may contribute to the quantum efficiency [9]. It was observed that the solar cell efficiency increases with increase in the CZTS absorber layer thickness.

However, it has a much slower increasing rate when the layer thickness is over 2500 nm. Therefore, thickness of 2500 nm is optimum to absorb most of the incident photons. Therefore, if one takes the processing times and material usage into account, fabricating the CZTS solar cells with thick absorber layer will not be very cost effective.

3.3 Effect of Series and Shunt Resistances

In order to obtain high efficiency solar cell, it is desirable to obtain low series resistance (R_s) and high shunt resistance (R_{sh}). Figure 6 represent current density (J)–voltage (V) and (b) quantum efficiency (QE)–wavelength (λ) curves to various series resistance (in $\Omega \text{ cm}^2$), respectively. The series resistance values were varied ($R_s = 1\text{--}6.5 \Omega \text{ cm}^2$). It was observed that open circuit voltage and short circuit current density gets reduced when we will increase series resistance, which further affect the fill factor of the devices. This was due to higher value of R_s directly effects the efficiency of PV cell. To obtain high efficiency of solar cells take low series resistance value (Fig. 7).

The power losses caused by the higher shunt resistance (R_{sh}) are typically due to the manufacturing defects. Low shunt resistance causes power losses in solar cells by providing an alternate current path for the light-generated current.

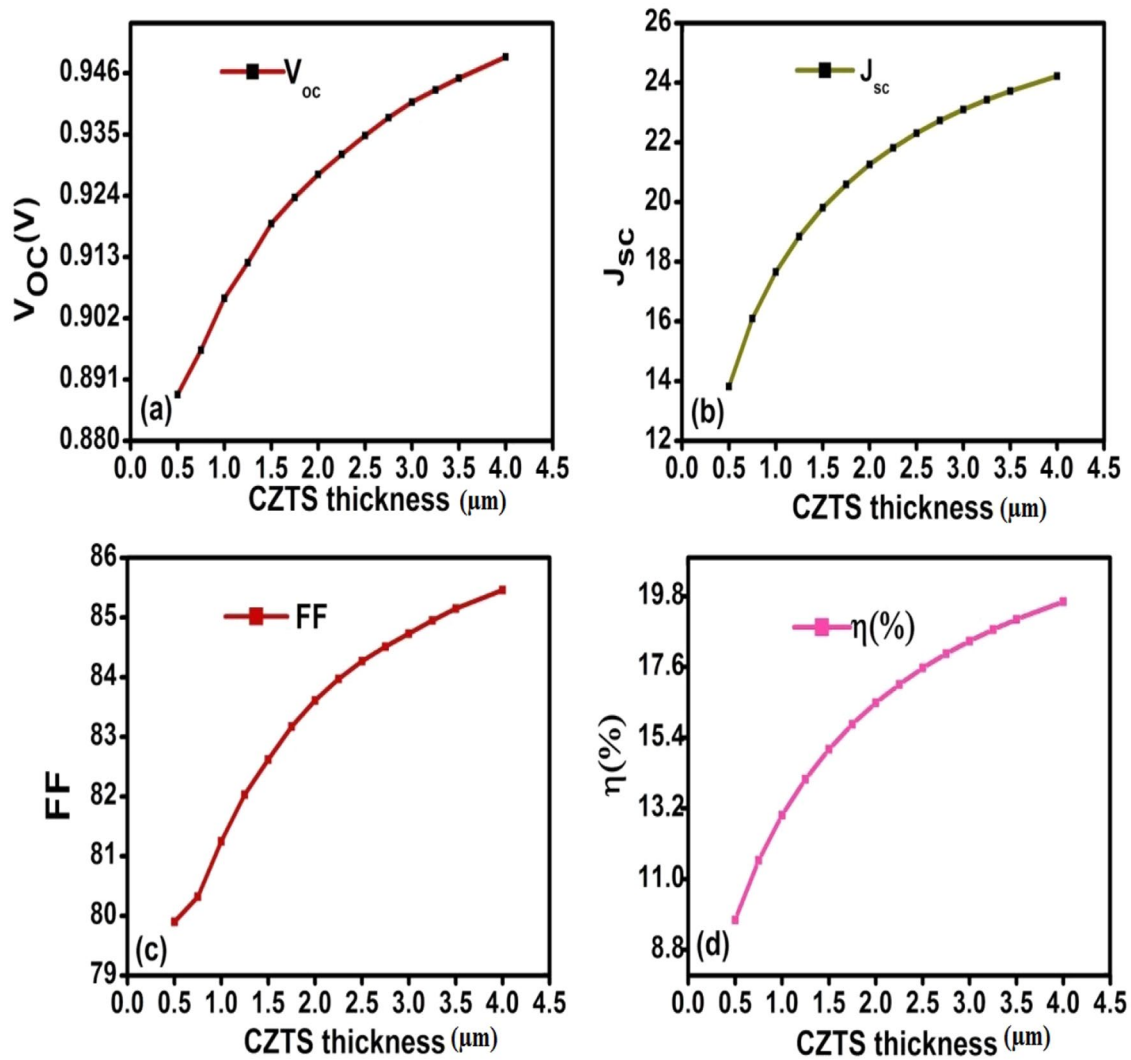


Fig. 5 a CZTS thickness effect on the cell V_{oc} , b CZTS thickness effect on the cell J_{sc} , c CZTS thickness effect on the cell FF, and d CZTS thickness effect on the cell η

Such a diversion reduces the amount of current flowing through the solar cell junction and reduces the voltage of the solar cell. Shunt resistance was inversely proportional to the fill factor [15]. Therefore, open circuit voltage will decrease, when we increase the shunt resistance. Even if R_s

assumed to be zero and R_{sh} infinitely large, it still not possible to have 100% fill factor, due to imperfect diode behavior of a solar cell. Based on the simulation results, the increase of R_s promotes bulk recombination [16].

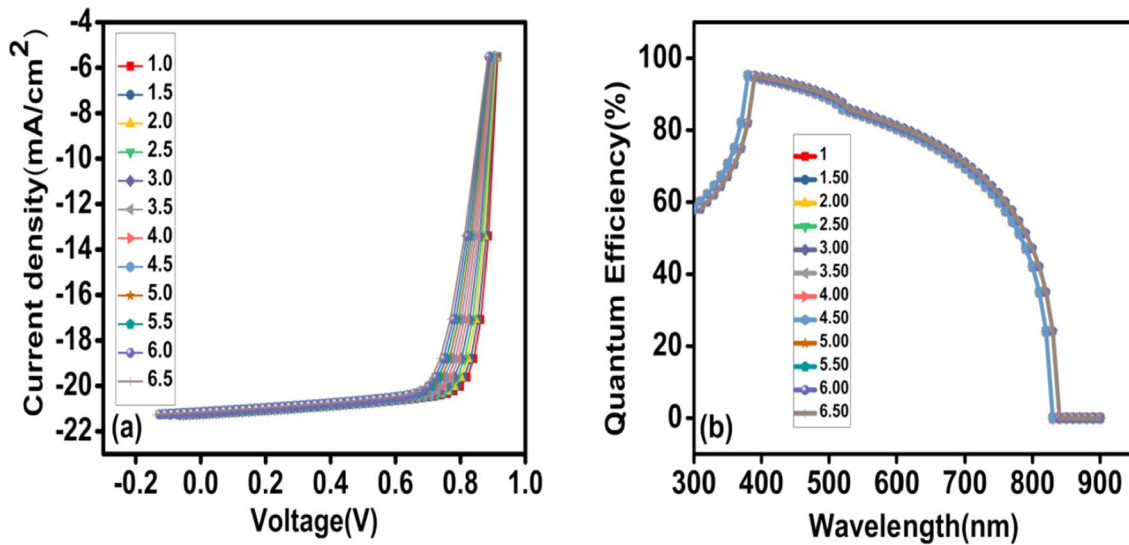


Fig. 6 a Current density (J)–voltage (V) and b quantum efficiency (QE)–wavelength (λ) curves according to different series resistance (in $\Omega \text{ cm}^2$)

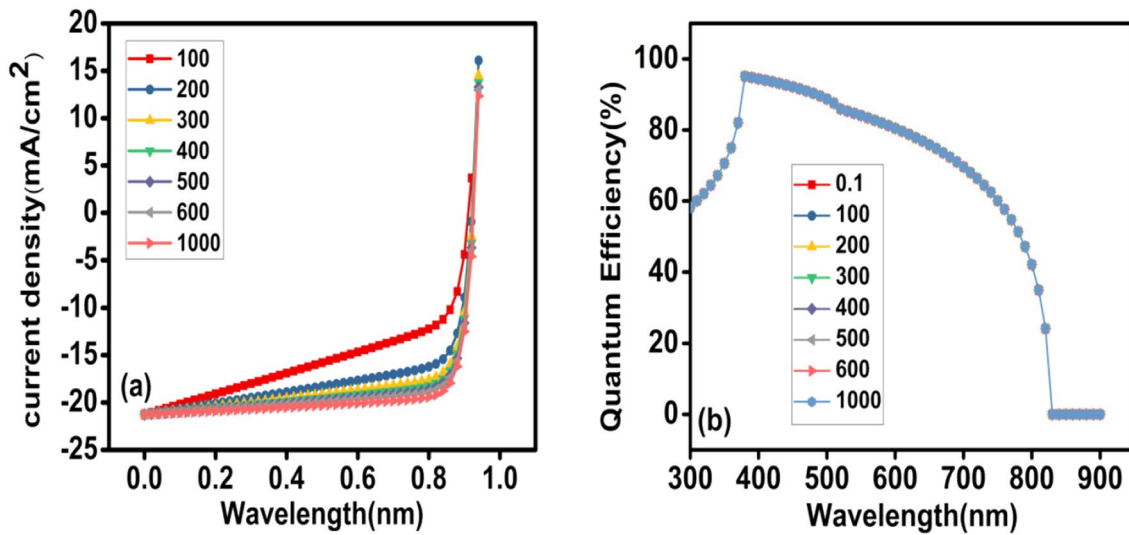


Fig. 7 a Current density (J)–voltage (V) and b quantum efficiency (QE)–wavelength (λ) curves according to different shunt resistance (in $\Omega \text{ cm}^2$)

4 Conclusion

In conclusion, the CZTS/CdS heterojunction solar cell performance was simulated using SCAPS-1D. In this paper, we have studied the influence of CZTS absorber layer thickness, temperature, series and shunt resistance on the performances of hetero-structure Mo/CZTS/CdS/ZnO. The simulated results show good performances, when the temperature of the CZTS absorber layer was at 280 K. For high efficiency of PV cell, optimum thickness of CZTS absorber layer was found to be at 2500 nm. High performances of PV cell were obtained, when the series and

shunt resistances is 1 $\Omega \text{ cm}^2$ and 1000 $\Omega \text{ cm}^2$, respectively. From the proposed structure, optical photovoltaic property has been achieved with an efficiency of 19.64% (with $J_{sc} = 24.22 \text{ mA/cm}^2$, $V_{oc} = 0.9489 \text{ V}$ and $FF = 86.13\%$).

References

1. S. Almosni, A. Delamarre, Z. Jehl, D. Suchet, L. Cojocaru, M. Giteau et al., Material challenges for solar cells in the twenty-first century: directions in emerging technologies. *Sci. Technol. Adv. Mater.* **19**, 336–369 (2018)

2. M.M. Rahaman, A. Chowdhury, M. Islam, M.M. Rahman, CZTS based thin film solar cell: an investigation into the influence of dark current on cell performance, in *2018 Joint 7th International Conference on Informatics, Electronics & Vision (ICIEV) and 2018 2nd International Conference on Imaging, Vision & Pattern Recognition (icIVPR)* (2018), pp. 87–92
3. M.P. Suryawanshi, G.L. Agawane, S.M. Bhosale, S.W. Shin, P.S. Patil, J.H. Kim et al., CZTS based thin film solar cells: a status review. *Mater. Technol.* **28**, 98–109 (2013)
4. S. Zhuk, D.A. Kushwaha, T. Wong, S. Masudy-Panah, A. Smirnov, G. Dalapati, Critical review on sputter-deposited $\text{Cu}_2\text{ZnSnS}_4$ (CZTS) based thin film photovoltaic technology focusing on device architecture and absorber quality on the solar cells performance. *Sol. Energy Mater. Sol. Cells* **171**, 239–252 (2017)
5. Y.H. Khattak, F. Baig, S. Ullah, B. Marí, S. Beg, H. Ullah, Enhancement of the conversion efficiency of thin film kesterite solar cell. *J. Renew. Sustain. Energy* **10**, 033501 (2018)
6. N. Song, M.A. Green, K. Sun, Y. Hu, C. Yan, X. Hao, Epitaxial growth of $\text{Cu}_2\text{ZnSnS}_4$ thin film on Si by radio frequency magnetron sputtering. *Appl. Phys. Lett.* **116**, 123901 (2020)
7. A. Ashery, I.M. El Radaf, M.M.M. Elnasharty, Electrical and dielectric characterizations of $\text{Cu}_2\text{ZnSnSe}_4/n\text{-Si}$ heterojunction. *Silicon* **11**, 2567–2574 (2019)
8. F.A. Jhuma, M.Z. Shaily, M.J. Rashid, Towards high-efficiency CZTS solar cell through buffer layer optimization. *Mater. Renew. Sustain. Energy* **8**, 6 (2019)
9. U. Mandadapu, V. Vedanayakam, K. Thyagarajan, B.J. Babu, Optimisation of high efficiency tin halide perovskite solar cells using SCAPS-1D. *Int. J. Simul. Process Model.* **13**, 221 (2018)
10. M. Burgelman, K. Decock, A. Niemegeers, J. Verschraegen, S. Degrave, *SCAPS Manual* (University of Ghent, Ghent, 2016)
11. M. Minbashi, M. Omrani, N. Memarian, D.-H. Kim, Comparison of theoretical and experimental results for band-gap-graded CZTSSe solar cell. *Curr. Appl. Phys.* **17**, 1238–1243 (2017)
12. M. Mohammed, H. Mazari, S. Khelifi, A. Bouraiou, R. Dabou, Simulation of high efficiency CIGS solar cells with SCAPS-1D software. *Energy Proc.* **74**, 736–744 (2015)
13. M. Patel, A. Ray, Enhancement of output performance of $\text{Cu}_2\text{ZnSnS}_4$ thin film solar cells—a numerical simulation approach and comparison to experiments. *Phys. B Condens. Matter* **407**, 4391–4397 (2012)
14. P. Singh, N. Ravindra, Temperature dependence of solar cell performance—an analysis. *Sol. Energy Mater. Sol. Cells* **101**, 36–45 (2012)
15. O.K. Simya, A. Mahaboobatcha, K. Balachander, A comparative study on the performance of kesterite based thin film solar cells using SCAPS simulation program. *Superlattices Microstruct.* **82**, 248 (2015)
16. M. Minbashi, A. Ghobadi, M. Ehsani, H. Dizaji, N. Memarian, Simulation of high efficiency SnS-based solar cells with SCAPS. *Sol. Energy* **176**, 520–525 (2018)

Publisher's Note Springer Nature remains neutral with regard to jurisdictional claims in published maps and institutional affiliations.